ASPS Conference Proceedings 1: 555-561 (20222)

Proceedings of

12th Structural Engineering Convention - An International Event (SEC 2022)

Available at https://asps-journals.com/index.php/acp

Effect of Skew Angle on the Dynamic Response of a Reinforced Concrete Bridge under Blast Loading

Roouf Un Nabi Dar[1, *], S.M. Anas[2], MehtabAlam[3]

[1]M. Tech Student;Department of Civil Engineering, Faculty of Engineering and Technology, JamiaMilliaIslamia, Jamia Nagar, New Delhi, Delhi, India – 110025
[2]Ph.D. Scholar; Department of Civil Engineering, Faculty of Engineering and Technology, JamiaMilliaIslamia, Jamia Nagar, New Delhi, Delhi, India – 110025
[3]Professor; Department of Civil Engineering, Faculty of Engineering and Technology, JamiaMilliaIslamia, Jamia Nagar, New Delhi, Delhi, India – 110025

Paper ID - 050387

Abstract

Accidental explosions and subversive blasts are on rise. The recent devastating Beirut explosion witnesses this fact. Performance of the structures such as bridges in cities and strategic boarder areas is of paramount importance. With this concern the effect of skew angle on the performance of a single span reinforced concrete (RC) bridge deck supported on three symmetrically placed RC girders under blast loading generated by1000kgTNT charge located above and below the mid-section of the central girder at a standoff distance of 0.5 m has been investigated using ABAQUS/CAE. Analyses have been performed at different skew angles i.e. 0º, 10º, 20º, 30º, 40º, and 50º. Several empirical relations from the literature have been used to estimate the blast parameters such as peak overpressure, positive phase duration, the arrival time of blast wave, and decay coefficient. Blast pressure P(t), has been modeled using modified Friedlander's equation. Distributions of damages have been evaluated with a mesh size of 300 mm using concrete damage plasticity (CDP) model. Maximum displacements have been computed and are compared with those obtained from the provisions of AASHTO: Load Resistance and Factor Design (LRFD) - Bridge Design Specifications (2014). It has been found that the midspan displacement and the stresses of the deck increase for 10º skew angle but decrease for subsequent increase in skew angle for the explosive charge loaded above the mid-section of the central girder. However, tensile as well as compressive damages in girders increase with increase of skew angle irrespective of the location of the blast. Side girders suffer more damage with increase in skew angle than uniform damage for 'under the deck' location of explosive charge.

Keywords: RCC Bridge; Skew angle, Blast; Damage; Cracks; CDP model; Finite element analysis.

1. Introduction

Tremendous growth in the construction of skew bridges especially in urban cities is seen now a days. All the bridges are not straight span. Straight span bridges are not always viable due to land/space constraint. However advanced construction technologies available facilitate to accommodate the geometric and space constraints and enables to construct the skewed bridges. Skewness of the bridge measured by skew angle (θ), can be defined as the angle between the axis of the bridge and the normal to the centerline of the abutment, as shown in Fig.1.

Considerable experimental and numerical studies have been conducted to examine the effect of skew angle on the dynamic behavior of RC bridges under different design loadings. (Meng J. and Lui M. E., 2000 [9]; Maleki S., 2002 [13]; Meng J. et al., 2004 [10]; Khasro M. and Kabir A. 2005; [8]. Demeke B. A. et al., 2006 [3]; Menassa C. et al.,2007 [11]; Kaliyaperumal G., 2010 [7]; Deepu S. P. et al. (2014) [4];Sharma M. et al., 2017 [16]; Sundria R. et al., 2019 [18]). Meng J. and Lui M. E., (2000) [9]numerically investigated the effects of structural flexibility, structural skewness, and boundary conditions on seismic response of reinforced concrete box girder bridge using Response Spectrum Method. It was concluded that the effect of the skew angle was more significant on the seismic response of RC bridge than other parameters considered. Maleki S., (2002) [13] conducted a parametric study of a single-span skewed reinforced concrete slab-girder bridges by varying the span length from 0 to 30 m and skew angle from 0º to 60º under seismic loading. The bridges were supported on elastomeric bearings in the longitudinal direction and with cross-frames in the skew direction. Linear response spectrum analysis was performed using SAP2000 software. It was concluded that the rigid deck can be used safely for skewed slab-girder bridges with spans up to 30 m and skews up to 60º. Meng J. et al., (2004) [10] experimentally studied the response of the RC skew bridge under vehicular loadings. The experimental results were compared with those obtained using SAP2000 program. They concluded that the finite element models were in close agreement withthe results of the test bridge. Khasro M. and Kabir A., (2005) [7] experimentally and numerically examined the response of RC skew slab under different vertical concentrated loads using a layered technique with skew angles of 25° and 45°. Prototypes of simply supported skew slabs were constructed on a scale of 1:6. The results were compared with those obtainedthrough the layered technique. Reasonable agreement was found between the numerical and the experimental results. They concluded that the load-carrying

*Corresponding author. Tel: +919891861190; E-mail address: malam1@jmi.ac.in

Published online: December 19, 2022
doi:10.38208/acp.v1.548

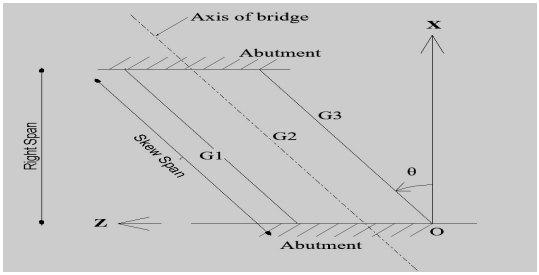

Fig.1: Skew bridge parameters

capacity of skew RC slabs decreased with the increase in skew angle. *Demeke B. A. et al., (2006) [3]* experimentally and numerically investigated the effects of vehicles-induced dynamic loads on a skew box reinforced girder bridge. A good agreement was found between the experimental and numerical results. The influence of skew angle on the behavior of the RC bridge was reported insignificant for skew angles in the range of 0º–30º. They observed that the width to span ratio of the deck played a significant role in determining the extent of influence of the skew on the behavior of the RC bridge. *Deepu S. P. et al. (2014) [4]* performed a numerical seismic vulnerability analysis of a typical highway overpass RC bridge with different skew angles. SAP2000 program was employed to carry out non-linear time-history analysis for the developed numerical models. Results indicated that the probability of failure increased with the increase in skew angle for a given ground motion intensity. Also, torsional coupling in all the skew models produced significant rotations (peak and residual both) which increased with an increase in the skew angle. *Sundria R. et al., (2019)[18]* numerically assessed the combined effect of slab width and skew angle on the performance of the RC deck under Class-A vehicular loading. 96 RC bridge decks were modeled using SAP2000 software. It was found that longitudinal moment decreased while transverse, torsional moments, and shear force increased with the increase in skew angle. They concluded that the torsional moment in a single lane bridge with a 50º skew angle was four times more than in straight bridge, while that in the four-lane RC bridge, was 2.76 times more than in the RC bridge with 0º skew angle.

The literature review reveals that the skew angle significantly influences the response of RC bridges under vehicular and seismic loadings. However, no investigation has been conducted to study the effect of skew angle on the behavior of RC bridges under blast loading. In the present study effect of to investigate the effect of skew angle on the performance of a single span RC bridge deck supported on three symmetrically placed girders under blast loading generated has been investigated using ABAQUS/CAE. Analyses have been performed considering skew angles of 0º, 10º, 20º, 30º, 40º, and50º. The computed maximum displacements have been compared with those obtained from the provisions of AASHTO: Load Resistance and Factor Design (LRFD) - Bridge Design Specifications (2014).Besides, crack patterns and percentage damages have been evaluated using the CDP model for the blast locations considered.

2. Numerical modeling

Deck of RC bridge is 0.23 m thick, has width of 9 m and skew span of 12 m. The deck is supported on three RC girders with spacing of 3 m. Clear cantilever projection of deck slab extending beyond side girders is of 1.255 m. Figure-2(a) shows the dimensions of the RC girder. The deck is reinforced with 12 mm diameter re-bars spaced at 125mm c/c as short-span positive as well as negative reinforcementand with 10 mm diameter re-bars at 125 mm c/c as long-span positive as well as negative reinforcement.Skewed models of RC bridge is shown in Figure-4. Average compressive strength, young's modulus, Poisson's ratio, and density of concrete are 30MPa, 27.30 GPa, 0.20, and 25 kN/m^3, respectively. The young's modulus and yield strength of steel are 200 GPa and 500 MPa. Rendered views of the finite element model of a straight bridge are shown inFigure-3. The contact between a deck and girders has been modeled using a kinematic constraint enforcement method with finite sliding which simulates the realistic contact between girders and deck.

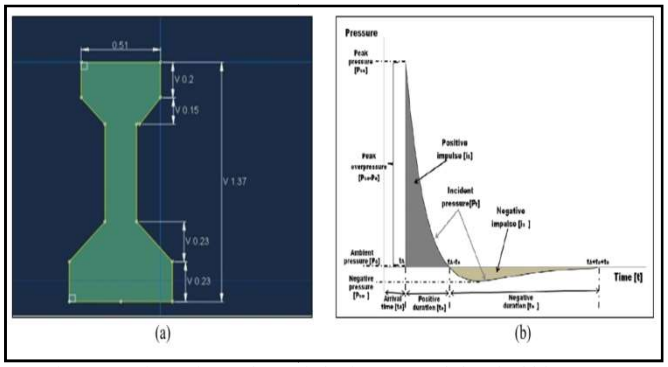

Fig.2: (a) Dimensions of RC girder in "m", and (b) Ideal blast wave pressure-time history

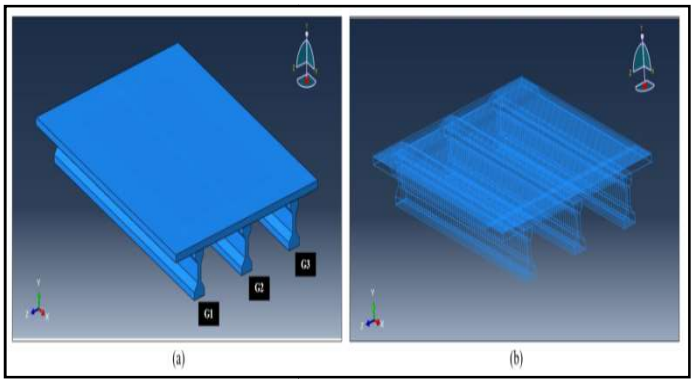

Fig.3: Rendered views of the model and reinforcement

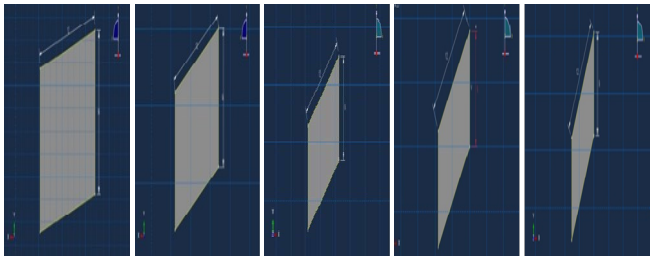

Fig.4: Different models of RC desk considered.

2.1. *Blast pressure – time history*

Figure-2 (b) shows the ideal blast wave pressure-time history. In general, the blast load is characterized by two phases namely, the positive pressure phase and the negative phase. The magnitude of peak pressure in the negative phase is much smaller than the positive phase (Figure-2(b)). IS 4991(1968) for *Criteria for Blast Resistant Design of Structures for Explosions Above Ground*[6]suggests that the effect of the negative phase on the performance of concrete structures should be neglected as it does not contribute to the response of the structure in blast analysis and design. Empirical equations proposed for peak overpressure (1) by Mills (1987) [12]; for positive phase duration (2) bySadovskiy M. A. et al. (2004) [15]; and for arrival time of blast wave (3) by Siddiqui J. I. et al. (2007) [17]have been used to estimate blast parameters such as peak overpressure, positive phase duration, and the arrival time of blast wave:

$$P_{so} = \frac{1.172}{Z^3} - \frac{0.114}{Z^2} + \frac{0.108}{Z} \quad (1)$$

$$t_d = 1.2 \times W^{1/6} \times \sqrt{R} \quad (2)$$

$$t_a = \frac{0.4 \times R^{1.2} \times W^{-0.2}}{340} \quad (3)$$

Where, P_{SO} = peak overpressure (MPa), t_d = positive phase duration (ms), t_a= arrival time of blast wave (ms), Z = scaled distance (m/kg$^{1/3}$), R = standoff distance (m), and W =amount of TNT (kg). The blast pressure-time history P(t), has been modeled using the modified Friedlander's equation given below [5]:

$$P(t) = P_o + P_{so} \times \left(1 - \frac{t}{t_d}\right) e^{-b\frac{t}{t_d}} \text{ (MPa)} \quad (4)$$

$$b = 1.5 \times Z^{-0.38} \quad (5)$$

Where, P_O = standard atmospheric pressure (0.1 MPa), and b = decay constant. Table-1 summarizes the calculated values of blast parameters. Fixed support boundary conditions are assigned to the ends of the girder to ensure they do not produce undue rotational displacement. RC bridge deck is assumed to act as a one-way restrained slab. Figure-6 shows the load applications of blast pressure for two locations of the explosive charge.

Table-1: Calculated values of blast parameters at Scaled distance of 0.05 m/kg$^{1/3}$

Standoff distance (m)	*Scaled distance (m/kg$^{1/3}$)*	*Peak overpressure (MPa)*	*Arrival time of blast wave (ms)*	*Positive phase duration (ms)*
0.5	0.05	9332	0.128	2.68

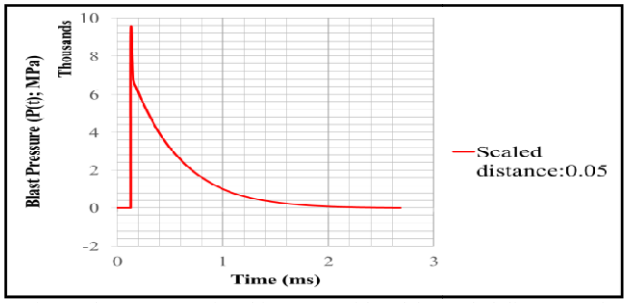

Fig.5: Blast pressure-time history considered for scaled distancee of 0.05*(m/kg$^{1/3}$)*

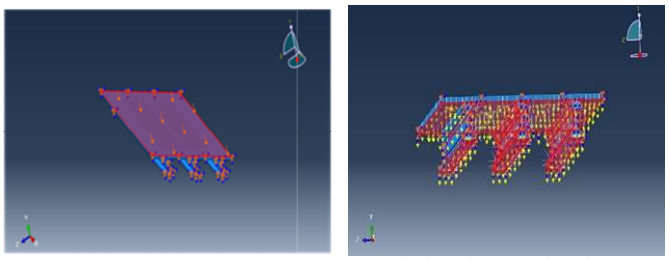

(a) above the central girder (b) below the central girder

Fig.6.: Load applications of blast pressure for different locations of the explosive charge considered

2.2. *Concrete damage plasticity model*

The concrete damage plasticity (CDP) model in ABAQUS/CAE provides a general capability of modeling concrete and other quasi-brittle materials in all types of structureal elements. It assumes that the main two failure criteria are tensile cracking and compressive crushing of the concrete material. The evolution of the yield (or failure) surface is controlled by two hardening variables, $\tilde{\epsilon}_t^{pl}$ and$\tilde{\epsilon}_c^{pl}$, linked to failure mechanisms under tension and compression, respectively. We refer to$\tilde{\epsilon}_t^{pl}$ and $\tilde{\epsilon}_c^{pl}$ as tensile and compressive equivalent plastic strains, respectively [1]. The model assumes that the uniaxial tensile and compressive response of concrete is characterized by damaged plasticity (see Figure 1).Under uniaxial tension, the stress-strain response follows a linear elastic relationship until the value of the failure stress, σ_{t0},is reached. The failure stress corresponds to the onset of micro-cracking in the concrete material. Beyond the failure stress, the formation of micro-cracks is represented macroscopically with a softening stress-strain response, which induces strain localization in the concrete structure. Under uniaxial compression, the response is linear until the value of initial yield σ_{c0}. In the plastic regime, the response is typically characterized by stress hardening followed by strain-softening beyond the ultimate stress σ_{cu}. This representation captures the main features of the response of concrete. The CDP properties for M30 grade concrete have been taken from Milad H. et al. (2015) [14]. For visualization of cracking, concrete damage plasticity assumes that the cracking starts at points where tensile equivalent plastic strain is greater than zero. Also, the direction of cracks as can be observed in the visualization mode of ABAQUS/CAE is taken parallel to the direction of plastic strain.

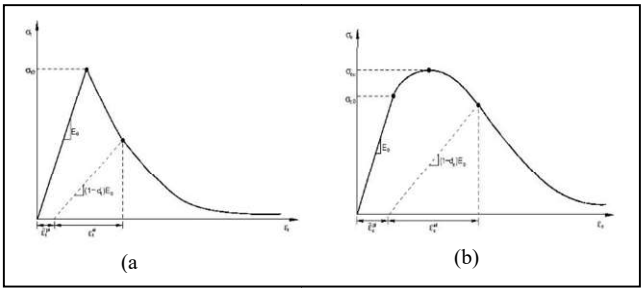

Fig.7: Response of concrete to uniaxial loading in tension (a) and compression (b).

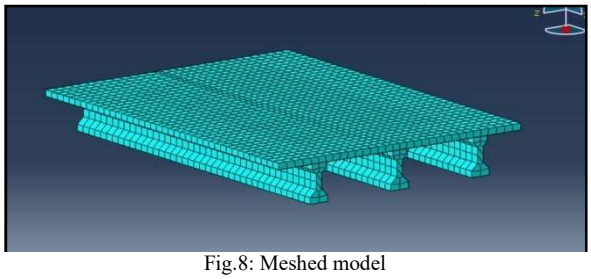

Fig.8: Meshed model

In this study, the explicit 8-noded brick element C3D8R element is used to model the concrete, while the re-bars have been modeled using a 2-noded truss element (T3D2). C3D8R element is a 3-dimensional linear brick element, fully integrated (2x2x2) integration points. T3D2 is a two-node, 3-dimensional truss element used in two and three dimensions to model slender, line-like structures that support only axial loading along with the element. Mesh convergence has been performed considering mesh size of 500mm, 450mm, 400mm, 350mm, 300mm and 250mm. Better convergence has been observed with 300 mm mesh size(Figure-8).

3. Results & discussion

Table-2 and 3 summarize the computed maximum displacements and von Mises stresses for the considered locations of the explosive charge. Fig.-9 and 10 show the distribution of resultant displacement and von Mises stress for the locations of explosive charge placed above the mid-section of the central girder. The maximum allowable displacements as per *AASHTO: LRFD Bridge design specifications (2014)* [2] is limited to L/1000, where "L" is the span of the deck slab i.e. 12mm in our case.When the explosive charge is placed above the deck at a scaled distance of 0.05 m/kg$^{1/3}$, the RC bridge deck with a 10º skew angle experienced a maximum resultant displacement of 6.3 mm which is greater than the displacement in straight span bridge (0º). However, the displacement is found to reduce thereafter for every 10º increase in skew angle (Table-2). Maximum displacement of 139 mm has been found corresponding to a skew angle of 50º
for below the deck location of the explosive charge. A similar trend has been observed for von Mises stresses. For blast placed above the bridge deck, bridge with 10º skew angle produced von Mises stress of magnitude 593 MPa greater than 540.4 MPa corresponding to straight span bridge. Thereafter increase in every 10º skew angle stress reduces the maximumstresses. The average percentagereduction in stress for every 10º increase in skew angle is calculated to be 7.5%.
Blast pressure applied above the deck has produced the maximum tensile damage of 2.5%, 3.1%, 5%, 5.5 and 6.5% in the deck corresponding to skew angles of 10º, 20º, 30º, 40º, and 50º respectively. Moreover, when blast pressure is applied below the deck, maximum tensile damage has been found to be 16%, 18%, 19%, 20%, and 25% for skew angles of 10º, 20º, 30º, 40º and 50º respectively as described in Table-4. No Compressive damage has been observed for blast location above the deck for all the considered skew angles.For blast location below the middle girder, compressive damage of 16%, 20%, 30%, 35%, and 40% have been found corresponding to 10º, 20º, 30º, 40º, and 50º skew angle, respectively.

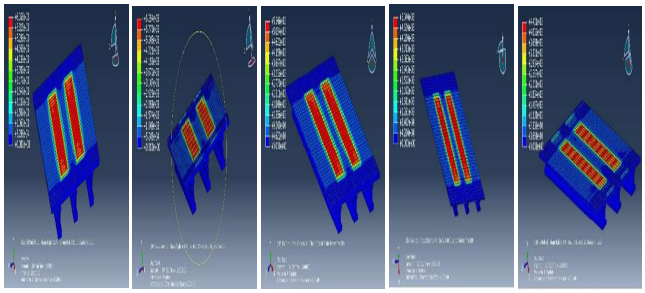

Fig.9: Resultant displacement distribution at a scaled distance of 0.05 m/kg$^{1/3}$ for different skew angles in "m"

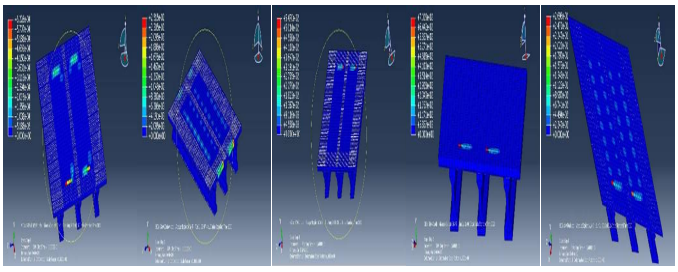

Fig.10: von Mises stress distribution at a scaled distance of 0.05 m/kg1/3 for different skew angles

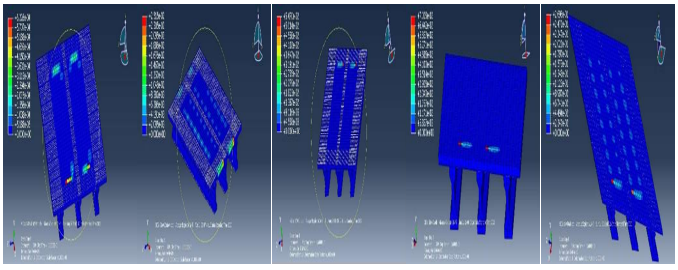

Fig.11: Compressive damage distribution at a scaled distance of 0.05 m/kg$^{1/3}$ with different skew angles for blast above the deck

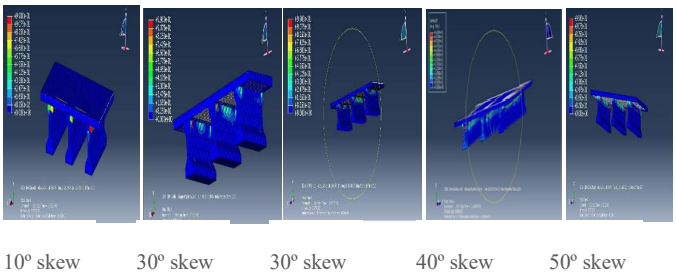

Fig.12: Tensile damage distribution at a scaled distance of 0.05 m/kg$^{1/3}$ with different skew angles for blast above the deck

. However, a straight modeled bridge has a suffered compressive damage of 37% for a blast below deckslab. Damage observed is small as compared to the straight bridge when the RC bridge was skewed 10º, and then increases thereafter (Table-4). Also, Table-5 gives detailed crack pattern for each considered case.

Table-2: Summary of computed maximum deformations and von-Mises stresses for the above deck location of blast

Skew Angle	*Maximum deformation (mm)*				*Maximum von Mises stress (MPa)*			
	Deck	G1	G2	G3	Deck	G1	G2	G3
0º	5.60	-	-	-	540.40	-	-	-
10º	6.36	-	-	-	593	-	-	-
20º	6.20	-	-	-	591	-	-	-
30º	5.54	-	-	-	523	-	-	-
40º	5.04	-	-	-	470	-	-	-
50º	4.40	-	-	-	416	-	-	-

Table-3: Summary of computed maximum deformations and von-Mises stresses for the below deck location of blast

Skew Angle	*Maximum deformation (mm)*				*Maximum von Mises stress (MPa)*			
	Deck (Corners)	G1	G2	G3	Deck (Corners)	G1	G2	G3
0º	7.5	6	12.4	6	650	500	709	500
10º	7	10	11	10	450	420	613	480
20º	6	13	13.0	13	420	490	845	500
30º	4.5	14	14.0	16	415	506	890	663
40º	1.4	15	17.9	17.9	380	515	900	770
50º	0	10	139	139	100	600	961	1049

Table-4: Tensile and compressive damage distribution

Skew Angle	*Location of blast*	*Percentage Damage (%)*	
		Tensile	*Compressive*
0º	Above the central girder	7.00 (G2); 3.00 (G1,3); 0.10 (Deck))	-
	Below the central girder	9 (G2); 13.00 (G1,3); 6.00 (Deck)	37.00 (G2); 18.00 (G1,3)
10º	Above the central girder	2.50 (G1,2); 1.25 (G3)	-
	Below the central girder	8 (G1,2); 1.00 (G3)	16(G1,2) 8(G3)
20º	Above the central girder	3.10 (G1,2,); 1.5(G3) 0.30 (Deck)	-
	Below the central girder	18 (G1,2); 1(Deck)	20 (G1,2); 2 (G3);
30º	Above the central girder	5 (G1,2); 3(G3) 1.5(Deck)	-
	Below the central girder	19 (G1,2) 2(Deck)	30 (G1,2)
40º	Above the central girder	5.5 (G1,2); 2.5 (G3); 2 (Deck)	-
	Below the central girder	20(G1,2) 2.5(Deck)	35 (G1,2)
50º	Above the central girder	6 (G1,2); 3(G3)	-
	Below the central girder	25(G1,2) 5 (Deck)	40(G1,2)

Table 5 Crack pattern

Skew Angle	*Location of blast*	*Remarks*
0º	Above the central girder	• Longitudinal tensile cracks in G2 girder in top junction at 1.8m from each end face of the girder. • Longitudinal cracks in the RC slab in L/3 portion near G1 and G3.
	Below the central girder	• Deep longitudinal tensile cracks in flange portion of girder. • Compression cracks at top and bottom flange penetrating the thickness of flanges in all the girders. • Heavy cracking in overhang portions of slab spaced less than 100mm apart.
10º	Above the central girder	• No tensile cracks in slab however transverse crack near the face of all the girders. • Minor transverse cracks between girders in the slab portion due to compression.
	Below the central girder	• Top flanges of G1, G3 girder found heavily cracked due to tension and longitudinal cracks 300mm deep found bottom web flange junctions of all girders.
20º	Above the central girder	• No tensile cracks in slab however cracks at the faces of G1 ,2 girder.
	Below the central girder	• 300 mm tensile cracks in the web of G1, G2 girders with little cracking in the deck. • Heavy cracking in web flange junctions of central girder and bottom flange junction of G, girder due to compression.
30º	Above the central girder	• Deep longitudinal tensile cracks in the flange portion of the girder G1,2,3. • No Compression cracks at top and bottom flange penetrating the thickness of flanges in all the girders. • Heavy cracking in overhang portions of slab spaced less than 100mm apart.
	Below the central girder	• Deep longitudinal tensile cracks at top and bottom junction in G1, G2 girders, and minor cracking in the top surface of the RC slab above girders due to tension. • Cracks spacing 300mm c/c and 150mm deep involving a bottom half portion of the web and bottom flanges in all the girders due to compression.
40º	Above the central girder	• Deep transverse tensile cracks in top flanges near faces in all girders. No tensile cracks in the central portion of girders. • Minor transverse cracks between girders in the slab portion due to compression.
	Below the central girder	• 0.3m deep longitudinal tensile cracks at top and bottom junction in G1, G2 girders, and minor cracking in the top surface of the slab • Cracks spacing 300mm c/c and 150 mm deep involving a bottom half portion of the web and bottom flanges in all the girders due to compression.
50º	Above the central girder	• Deep longitudinal tensile cracks in top flanges in all girders. • Minor transverse crack between girders in the slab portion due to compression.
	Below the central girder	• Heavy tensile cracking in the top and bottom flanges in all girders and the top surface of the RC slab above girders • Heavy cracks found in bottom flanges of all girders and cracks in the top flange of the central girder due to compression.

4. Conclusions

Analyses have been performed on a single span bridge with three girders and cantilevered deck subjected to a high explosive charge of 1000kg (TNT) above and below the mid-span section of the central for skew angles of 10º, 20º, 30º, 40º, and 50º. Results have been compared with the straight span bridge. Based on the results of the analyses, the following conclusions can be drawn:

When blast is above the deck

It has been found that the midspan deflection and the von Mises stresses of the deck increase for 10º skew angle but decrease for subsequent increase in skew angle for this case. Maximum displacement of 4.4 mm corresponding to skew angle of 50º is the least deflection found of all the skew angles considered. No tensile damage in the deck is observed upto 20º skew angle. Subsequent increase in skew angle resulted in tensile damage in the deck producing maximum damage of5% for 50º skew. No compressive damage in the deck is reported for blast located above the deck.

No displacement and von Mises stress have been reported in all the girders for this case. However, for 10º skew angle tensile damage in Girder 1 and 2 is more than in girder Girder 3. But damage in each girder is less than the case of straightmodeled bridge. With further increase in skew angle damage in Girder 1 will keep on increasing and has maximum value of 25% in G1,2 and 3% in G3 with skew angle of 50.º No compressive damage in girders is reported for blast located above the deck. For blast located above the deck, the RC bridge is found to be safe from the deflection point of view.

When blast is below the deck

For blast pressure applied below the deck, the deflections and stresses decrease for every 10º increase in skew angle. Tensile damage in the deck first reduces for10º skew angle then increases in subsequent increase in skew angle producing maximum damage of 5% with 50º skew angle. No compressive damage has been found in the deck.

Deflections and stresses first reduce with 10º for G2 girder then increase with increase in skew angle. These parameters are found to increase with increase in skew angle for G2,3 girders. For 10º skew angle compression damage in Girder 1 and 2 is more than in girder G 3. However damage in each girder is less than the case of straight modeled bridge. With further increase in skew angle damage in girder 1 will keep on increasing and has maximum value of 40% with skew angle of 50º. Percentage compression damage in the side girder G3 decreases with 20º skew angle to a value of 2% and for subsequent increase in skew angle damage in G3 becomes zero. Top and bottom web flange junctions are likely to suffer maximum damage in every skewed geometry considered. For the below deck location of the blast with 50º skew, the RC bridge is found to be unsafe.

5. Acknowledgement

The research work is a part of my post-graduation program. I owe this work to Prof. T. K Dutta (Department of Civil Engineering, Indian Institute of Technology Delhi, Delhi) for his genuine help and guidance. Besides, the facilities and resources provided by Department of Civil Engineering, Jamia Millia Islamia, New Delhi has been of immense help. I also extend my gratitude to fellow scholars for the kind of loving inspiration and genuine help in carrying out this research.

Disclosures

Free Access to this article is sponsored by SARL ALPHA CRISTO INDUSTRIAL.

6. References

[1] ABAQUS 6.14. User Documentation, Dessault Systems, 2014.

[2] AASHTO. Load resistance and factor design: Bridge design specifications. Seventh edition. *American association of state highway and transportation officials*, Washington D.C. 2014

[3] Demeke B. A., Chan T. H. T., and Yu L. Evaluation of dynamic loads on a skew box girder continuous bridge part II: parametric study and dynamic load factor. *Engineering structures*, 2007; 29(6):1064–73.

[4] Deepu S. P.,Prajapat K., and Chaudhuri R. S.Seismic vulnerability of skew bridges under bi-directional ground motions. *Engineering Structures*, 2014; 71. 150–160. 10.1016/j.engstruct..04.013.

[5] Dewey J. The Friedlander equations. 10.1007/978-3-319-70831-7_3, 2018.

[6] IS: 4991-1968 Criteria for blast resistant design of structures for explosions above ground. Third Reprint AUGUST 1993, UDC 699.85:624.04

[7] Kaliyaperumal G., ImamB., and Righiniotis T.Advanced dynamic finite element analysis of a skew steel railway bridge. *Engineering Structures*, 2011; 33 181–190

[8] Khasro M. and Ahsanul K.A Study on Reinforced Concrete Skew Slab Behavior. *J. of Civil Eng.,* 2005; Vol. 33, No. 2, pp. 93-101.Meng J. and Lui M. E. Seismic analysis and assessment of a skew highway bridge. *Engineering Structures*. 2000; 22,1433–1452.

[9] Meng J., Ghasemi H., and Lui E. M.Analytical and experimental study of a skew bridge model. *Engineering Structures*, 2004; 26:1127–42.

[10] Menassa C., Mabsout M., Tarhini K.and Frederick G.Influence of Skew Angle on Reinforced Concrete Slab Bridge. *Journal of Bridge Engineering,* 2007; Vol. 12, No. 2, ©ASCE, ISSN 1084-0702/2007/2-205–214

[11] Mills C. A. The design of concrete structures to resist explosions and weapon effects. *Proceedings of the 1st Int. Conference on concrete for hazard protections*, 1987;Edinburgh, UK.Maleki S. Deck modeling for seismic analysis of skewed slab-girder bridges.*Engineering Structures.*,2002; 24.1315–1326

[12] Milad H., Hijazi F., Vaghei R., and Jaafar M. S. Simplified Damage Plasticity Model for Concrete. *Structural EngineeringInternational*,2017;Nr.1.DOI:10.2749/101686616X1081.

[13] Sadovskiy M. A.Mechanical effects of air shockwaves from explosions according to experiments.*Sadovskiy MA Selected Works: Geophysics and Physics of Explosion*, 2004; Nauka Press, Moscow, Russia.

[14] Sharma M., Naveen K., and Singh H. Skew Slab Bridges—A Review. *Int. J. Civil Engg. Conc.Struct.*, 2017;Vol. 2, No. 3.

[15] Siddiqui J. I. and Ahmad S. Impulsive loading on a concrete structure. *Proceedings of the Institution of Civil Engineers, Structures and building,* 2007; 160.

[16] Sundria R. and Tripathi R. K.Effect of skewness on reinforced Concrete slab bridge by finite element method. *International Journal of Bridge Engineering (IJBE),* 2019; Vol. 7, No. 1, pp. 33-40.

[17] TM 5-1300/NAVFAC P-397/AFR 88-22. Structures to Resist the Effects of Accidental Explosions*. U. S. Departments of the Army, Navy, and Air Force*, 1990).